Bandgap characteristics of 2D plasma photonic crystal with oblique incidence: TM case*

Xie Ying-Tao(谢应涛)[a)] and Yang Li-Xia(杨利霞)[a)b)†]

[a)] *Department of Communication Engnerring, Jiangsu University, Zhenjiang* 212013, *China*

[b)] *State Key Laboratory of Millimeter Waves, Southeast University, Nanjing* 210096, *China*

(Received 20 October 2010; revised manuscript received 23 February 2011)

A novel periodic boundary condition (PBC), that is the constant transverse wavenumber (CTW) method, is introduced to solve the time delay in the transverse plane with oblique incidence. Based on the novel PBC, the FDTD/PBC algorithm is proposed to study periodic structure consisting of plasma and vacuum. Then the reflection coefficient for the plasma slab from the FDTD/PBC algorithm is compared with the analytic results to show the validity of our technique. Finally, the reflection coefficients for the plasma photonic crystals are calculated using the FDTD/PBC algorithm to study the variation of bandgap characteristics with the incident angle and the plasma parameters. Thus it has provided the guiding sense for the actual manufacturing plasma photonic crystal.

Keywords: finite-difference time-domain method, photonic crystal, plasma, periodic boundary condition

PACS: 02.70.–c, 95.75.Pq **DOI:** 10.1088/1674-1056/20/6/060201

1. Introduction

Generally, periodic structures are periodic in one or more dimensions and are used in applications, such as the design of antenna radomes, sub-reflectors for dual frequency reflector antenna systems and optic and infrared filters due to their own unique characteristics. For instance, the early frequency selective surfaces (FSS) which are a type of the periodic structures and the recently arising electromagnetic bandgap (EBG) or photonic bandgap (PBG) which possesses the excellent characteristic of controlling the electromagnetic or optic waves and has been the focus of many research fields. It has become more important for studying the periodic structures in practical application and theory.

To analyse the electromagnetic characteristics of this periodic structure, numerical methods that can readily handle a complex, inhomogeneous medium are required. So far the finite-difference time-domain (FDTD)[1] algorithm generally has been applied to solve this problem in that the FDTD grid needs only to be applied to a single-unit cell of the structure with the periodic boundary condition (PBC), making the analysis of a large structure much simpler and more computationally efficient than the modeling of the entire structure.

The method for implementing the PBC in the time domain is important. For a normally incident wave,[2] implementing the PBC is straightforward because there is no time delay between periodic cells. However, when a plane-wave source is obliquely incident, there is a time delay caused by cell-to-cell phase variation in frequency domain between corresponding points in different unit cells which causes the time-domain implementation to become more difficult. In order to solve this problem, several techniques have been proposed. The types of these techniques are the sin–cosine technique[3] and the split–field technique.[4] In the sin–cosine technique, the structure is excited once by a sine signal and once by a cosine signal. The PBC for the oblique incidence can be well implemented by an appropriate combination of these two excitations in an appropriate way. This method

*Project supported by the National Natural Science Foundation of China (Grant No. 61072002), the Ph. D. Program Foundation of the Ministry of Education of China (Grant No. 20093227120018), the Science and Techniques Planning Project of Jiangsu Province of China (Grant No. BE2008107), the Opening Funding of the State Key Laboratory of Millimeter Waves (Grant No. K200910), the Advanced Professional Scientific Research Foundation of Jiangsu University (Grant No. 07JDG063), and the 9th Undergraduate Research Foundation of Jiangsu University (Grant No. 09A044).

†Corresponding author. E-mail: lixiayang@yeah.net

© 2011 Chinese Physical Society and IOP Publishing Ltd

is a single frequency technique and loses the wide-band capability of the FDTD because of the sine and cosine excitations. In the split–field technique, extra terms are added to eliminate the time delay in the transverse plane. However, because of these extra terms, one needs to split the fields and uses a multi-part algorithm to implement FDTD, which adds to the complexity of the problem. Recently, spectral FDTD (SFDTD) method complements the conventional single-angle incident wave, with a constant transverse wavenumber (CTW) wave. The advantage of the method is that it is straightforward as in how to change an existing FDTD code to an SFDTD code and a wide-band frequency approach as compared to that of sin–cosine which is single frequency.

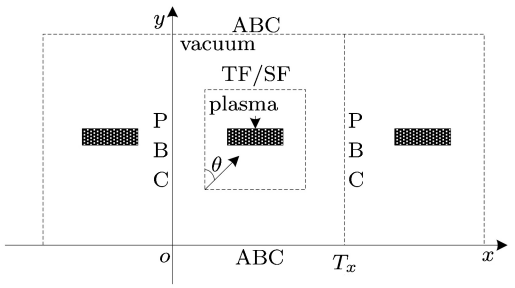


Fig. 1. Cross section view of a plane wave obliquely incident on a periodic structure consisting of plasma and vacuum, where T_x is the periodicity, θ is the incident angle, the background is vacuum and the scattered object is plasma, ABC is the absorbing boundary condition, PBC is the periodic boundary condition, TF/SF is the total-field/scattered field.

In this paper, we focus on studying the bandgap characteristics of the periodic structures consisting of plasma and vacuum, i.e. plasma photonic crystal (PPC), as shown in Fig. 1. First of all, we simply present the SFDTD method as in Refs. [5] and [6] and then introduce the FDTD technique which was developed to deal with the plasma in the published paper.[7−9] Afterwards we combine the SFDTD method with the published FDTD techniques to propose FDTD/PBC algorithm to study the characteristics of PPCs and then verify its validation by comparing it with the analytic results for the plasma slab. Finally, the reflection coefficients for the plasma photonic crystals[10−15] using the FDTD/PBC algorithm are calculated to study the bandgap characteristics as the incident angle and the plasma parameters are changed and some useful and interesting conclusions can be obtained.

2. FDTD/PBC algorithm

2.1. Spectral FDTD implementation

All periodic boundary conditions are developed based on the Floquet theory.[16] For a periodic structure with periodicity T_x along the x direction in Fig. 1, electromagnetic fields at the two boundaries $x = 0$ and $x = T_x$ satisfy the following equations in the frequency domain

$$\begin{aligned} \boldsymbol{E}(x=0,y,z,\omega) &= \boldsymbol{E}(x=T_x,y,z,\omega)\mathrm{e}^{\mathrm{j}k_xT_x}, \\ \boldsymbol{H}(x=0,y,z,\omega) &= \boldsymbol{H}(x=T_x,y,z,\omega)\mathrm{e}^{\mathrm{j}k_xT_x}. \end{aligned} \tag{1}$$

The exponential term represents a propagation phase delay in Eq. (1), which is determined by the propagation constant k_x and the periodicity T_x.

For a given incident angle in conventional ideas, the propagation constant k_x is known, which is determined by the frequency and incident angle $k_x = k_0 \sin\theta = 2\pi f\sqrt{\mu_0\varepsilon_0}\sin\theta$. It is difficult to implement the PBC in time domain because of the time delay. However, now we assume the transverse wave number k_x is constant, i.e. independent of the angular frequency ω. According to the inverse Fourier transform, equation (1) can be written as

$$\begin{aligned} \boldsymbol{E}(x=0,y,z,t) &= \boldsymbol{E}(x=T_x,y,z,t)\mathrm{e}^{\mathrm{j}k_xT_x}, \\ \boldsymbol{H}(x=0,y,z,t) &= \boldsymbol{H}(x=T_x,y,z,t)\mathrm{e}^{\mathrm{j}k_xT_x}. \end{aligned} \tag{2}$$

For Eq. (2), the time delay does not exist and it can be easily implemented similarly to the PBC with the normal incidence.

As an example of the TMz mode, the incidence of the approaching wave on a periodic structure, the tangential component of incident electromagnetic wave can be expressed as follows:

$$\begin{aligned} E_z^{\mathrm{inc}} &= E_0, \\ H_x^{\mathrm{inc}} &= -\frac{E_0}{\eta}\cos\theta = -\frac{E_0}{\eta}\sqrt{1-(k_x/k_0)^2}, \end{aligned} \tag{3}$$

where η is impedance in vacuum.

It is well known that one important issue related to the proposed algorithm is the excitation of plane waves in the computational domain. Unlike the traditional total-field/scattered field technique, only the E_z component is added on the excitation plane for the TMz case because according to Eq. (3), the H_x component depends on the incident angle. As a consequence of the one-field excitation technique, the plane wave is excited to propagate along both the upper and the lower regions. Thus, the entire computational domain becomes the total field region and there is no scattered

field region. The scattered field can be calculated by the difference of total field and the incident field.

Similar strategy applies to TEz case. The incident field adopts a modulated Gaussian waveform and the phase delay along the x direction should be inserted

$$E_z^{\rm inc}(x,t) = \exp\left[-\frac{(t-t_0)^2}{2\sigma_t^2}\right] \times \exp(\mathrm{j}2\pi f_0 t)\exp(-\mathrm{j}k_x x), \quad (4)$$

where the parameter

$$\sigma_t = \frac{3}{\pi \times \omega_{\rm BW}},$$

$\omega_{\rm BW}$ is the frequency bandwidth, the time delay $t_0 = 3\sigma_t - 5\sigma_t$, the centre frequency

$$f_0 = k_x c_0/2\pi + \omega_{\rm BW}/2,$$

c_0 is the free space wave speed.

2.2. Derivation of FDTD formula for plasma

In TMz case, Maxwell equations and constitutive relation for cold plasma are given by

$$\begin{cases} \dfrac{\partial E_z}{\partial y} = -\mu_0 \dfrac{\partial H_x}{\partial t}, \\ \dfrac{\partial E_z}{\partial x} = \mu_0 \dfrac{\partial H_y}{\partial t}, \\ \dfrac{\partial H_y}{\partial x} - \dfrac{\partial H_x}{\partial y} = \varepsilon_0 \dfrac{\partial E_z}{\partial t} + J_z, \\ \dfrac{\mathrm{d}J_z}{\mathrm{d}t} = \varepsilon_0 \omega_p^2 E_z - v J_z. \end{cases} \quad (5)$$

We may put J_z and E_z on the same node, then we have

$$H_x|_{i,j+1/2}^{n+1/2} = H_x|_{i,j+1/2}^{n-1/2} - \frac{\Delta t}{\mu_0}\frac{E_z|_{i,j+1}^n - E_z|_{i,j}^n}{\Delta y}, \quad (6)$$

$$H_y|_{i+1/2,j}^{n+1/2} = H_y|_{i+1/2,j}^{n-1/2} + \frac{\Delta t}{\mu_0}\frac{E_z|_{i+1,j}^n - E_z|_{i,j}^n}{\Delta x}, \quad (7)$$

$$E_z|_{i,j}^{n+1} = E_z|_{i,j}^n + \frac{\Delta t}{\varepsilon_0}\left[\frac{H_y|_{i+1/2,j}^{n+1/2} - H_y|_{i-1/2,j}^{n+1/2}}{\Delta x} - \frac{H_x|_{i,j+1/2}^{n+1/2} - H_x|_{i,j-1/2}^{n+1/2}}{\Delta y}\right] - \frac{\Delta t}{\varepsilon_0} J_z|_{i,j}^{n+1/2}. \quad (8)$$

According to Refs. [7]–[9], using the CDLT–FDTD algorithm, we can easily obtain

$$J_z|_{i,j}^{n+1/2} = \mathrm{e}^{-v\Delta t} J_z|_{i,j}^{n-1/2} + \varepsilon_0 \omega_p^2 \Delta t \mathrm{e}^{-v\Delta t/2} E_z|_{i,j}^n. \quad (9)$$

2.3. Numerical results

In order to validate the accuracy of the above FDTD algorithm, the novel FDTD is applied to calculate the TMz reflection coefficients for the plasma slab of 9 mm in thickness. This structure is chosen because the plasma slab can be considered as a periodic structure with arbitrary periodicity and the analytical results[17] are available. In the calculation, the FDTD grids have a spatial cell of $\delta = 0.25$ mm and a time step of $\mathrm{d}t = \delta/2c$. The frequency bandwidth BW is 20 GHz in the source.

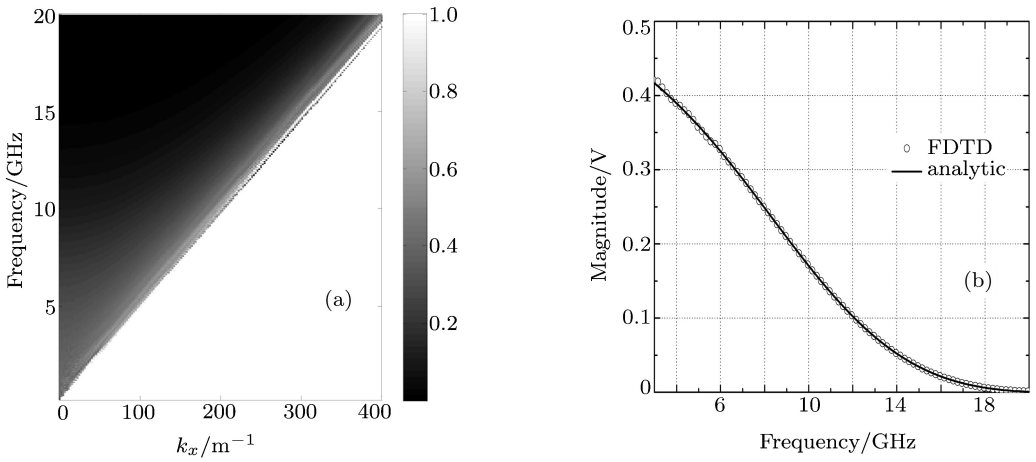


Fig. 2. Power reflection coefficients of the plasma slab, (a) the k_x-frequency plane and (b) the results of analytic and FDTD.

The plasma parameters are $\omega_{\rm p} = 50$ GHz, $\nu = 20$ GHz. Reflection coefficients in the k_x-frequency plane are calculated at 200 different k_x values ranging from 0 to 448 (radian/m), as shown in Fig. 2(a). In order to clarify the physical meaning, the curves of the reflection coefficient versus frequency at given incident angles can be extracted from the reflection coefficient data on k_x-frequency. For given incident angle θ and frequency f, the transverse wavenumber k_x can be calculated from $k_x = \omega\sqrt{\mu\varepsilon}\cos\theta$. Assuming that k_{x1} and k_{x2} ($k_{x1} \le k_x < k_{x2}$) are sampled transverse wavenumbers closest to k_x, the reflection coefficient $\Gamma(k_x, f)$ can be calculated by the following equation

$$\Gamma(f, k_x) = \{\Gamma(f, k_{x1}) \cdot (k_{x2} - k_x) + \Gamma(f, k_{x2}) \cdot (k_x - k_{x1})\}/(k_{x2} - k_{x1}). \quad (10)$$

The reflection coefficient for the incident angle of 30° extracted and plotted in Fig. 2(b). From Fig. 2(b), the results obtained by the FDTD/PBC method are compared with the analytical reflection coefficients, showing that the technique is correct and efficient.

3. Study of bandgap of 2D PPC in oblique incidence

To investigate the bandgap characteristics of PPC with the FDTD/PBC algorithm, we consider an FDTD computational geometric model shown in Fig. 3, where ε_0 is the permittivity of vacuum. In the model, six identical plasma scatterers of rectangular configuration are set in free space to constitute plasma photonic crystal. Electromagnetic wave illuminates the photonic crystal from top to bottom. The scatterers are composed of six rows of 4-mm-length ($d = 4$) squares with the period $T_x = 11.5$ mm, other parameters related to FDTD simulation are defined as in Subsection 2.3.

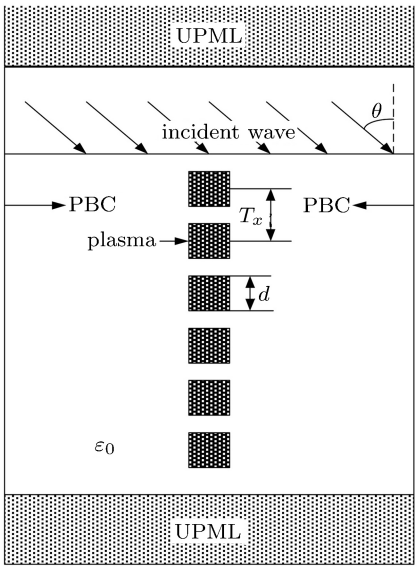
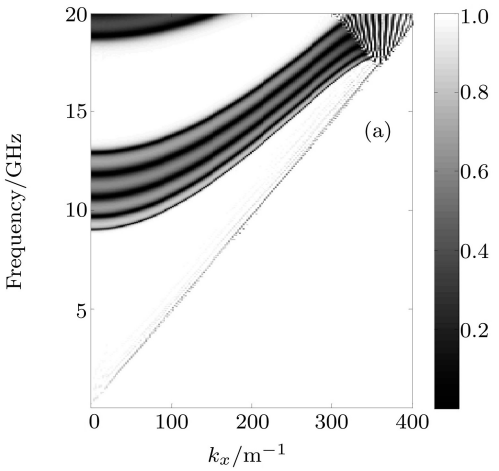


Fig. 3. Simulation configuration of the periodic structure by FDTD method. In this figure, T_x is the periodicity, θ is the incident angle, ε_0 is the permittivity of vacuum, UPML is the uninitial perfectly matched layer and PBC is the periodic boundary condition.

3.1. Effects of incident angle

In the calculation, we set $v = 0$ GHz, $\omega_{\rm p} = 250$ GHz for the plasma. The reflection coefficient of the 2D-PPC in the k_x-frequency plane computed using the FDTD/PBC algorithm is shown in Fig. 4(a). Figure 4(b) shows the change of reflection coefficients with incident angles for TMz mode.



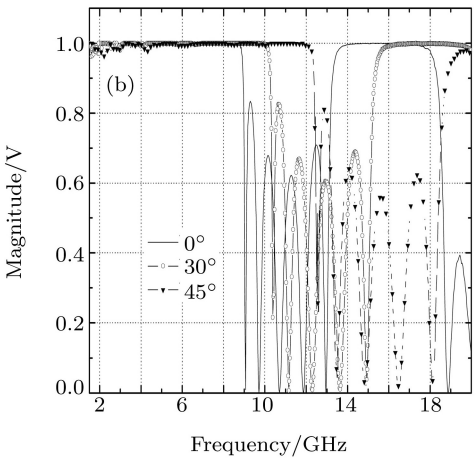


Fig. 4. Power reflection coefficient of the 2D-PPC, (a) k_x-frequency plane and (b) incident angles $\theta = 0°$, 30°, and 45°.

Similar to the example of validation, the power reflection coefficient of the 2D-PPC in k_x-frequency plane are first calculated by the FDTD/PBC algorithm and then the power reflection coefficients of the 2D-PPC at given incident angles are extracted. In Fig. 4(b), considering the frequency, at which the reflection coefficient equals unity, as the photonic bandgap, for the incident angle $\theta = 0$, the 2D-PPC can lead to two bandgaps with 20 GHz: the first one lies approximately between 0 and 8.9 GHz and the second one is approximately between 13.2 GHz and 17.4 GHz. When the incident angle $\theta = 30°$, there are still two bandgaps with 20 GHz. However, both of the cutoff frequency are broadened into high frequency region, the upper cutoff frequencies of the first one becomes 9.9 GHz and the lower and upper cutoff frequencies of the second one become 15.4 GHz and 19.6 GHz respectively. In addition, the centre frequencies of the two bandgaps are also broadened into high frequency region obviously. As for $\theta = 45°$, the similar trend exists and the upper cutoff frequency of the first one further increases to 11.8 GHz, yet the cutoff frequency of the second one increases beyond 20 GHz. According to the band structures above, it is found that the incident angle in PPC can enlarge the centre and cutoff frequencies of the gaps whatever are the first one and the second one. Therefore, the influence of incident angle must be taken into account while designing PPC devices. Physically, according to the electromagnetic theory, as the incident angle varies, the wave impedance must be changed. Then, the reflection coefficient must be changed, i.e. changes the bandwidth.

3.2. Effects of plasma frequency

Figure 5 shows the variation of reflection coefficients with plasma frequency for TMz mode with $\theta = 30°$ and $45°$. In the calculation, we set $v = 0$ GHz for the plasma.

From Fig. 5(a), for incident angle $\theta = 30°$, the bandwidths of the first and second forbidden bands are both broadened with increasing plasma frequency. For $\omega_p = 150$ GHz, the first bandgap lies between 0 GHz and 6.8 GHz, when the plasma frequency increases to 200 GHz and 250 GHz, the upper cutoff frequency corresponding to the first bandgap enlarges to 8.4 GHz and 9.9 GHz. As for the second one, it is not obvious at $\omega_p = 150$ GHz, while enlarging the plasma frequency to 200 GHz and 250 GHz, there exists obvious bandgap. The lower cutoff frequency almost does not vary with the difference of the plasma frequencies, which are both about 15.8 GHz for $\omega_p = 200$, 250 GHz, yet the upper cutoff frequencies broaden into high frequency, which is about 17.5 GHz and 20.1 GHz for $\omega_p = 200$, 250 GHz respectively. From Fig. 5(b), at incident angle $\theta = 45°$, similar trend exists. Physically, the relative permittivity of the plasma is $\varepsilon_r = 1 - \omega_p^2/\omega^2$. As ω_p varies, the corresponding ε_r must change. So the change of the bandwidth is reasonable.

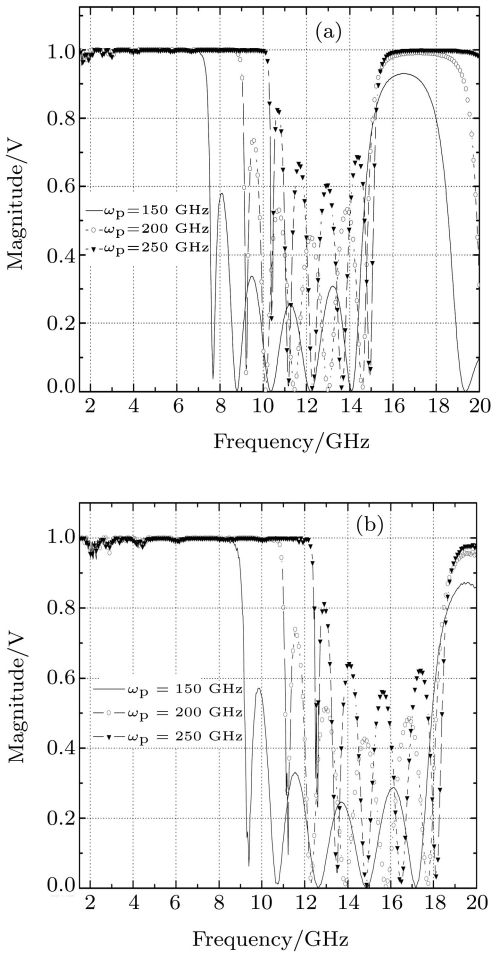


Fig. 5. Power reflection coefficients of the 2D-PPC with $\omega_p = 150$, 200 and 250 GHz at different incident angles, (a) $\theta = 30°$ and (b) $\theta = 45°$.

3.3. Effects of plasma collision frequency

Figure 6 shows the change of reflection coefficients with plasma collision frequency for TMz mode at $\theta = 30°$ and $45°$. In the calculation, we set $\omega_p = 150$ GHz for the plasma.

From Fig. 6, the curve of reflection coefficients tends to be flat with increasing plasma collision frequency, that is, the fluctuation range of the magnitude becomes smaller and the peak tends to zero. As a re-

sult, the photonic bandgap vanishes gradually. Physically, it could be explained on the basis that the larger the plasma frequency increases, the more the electromagnetic wave energy is absorbed to transfer its own quantity of heat. The total of the electromagnetic wave energy are invariable, consequently the magnitude of reflection coefficients must become smaller. In conclusion, increasing the plasma frequency is impossible to broaden the bandwidth.

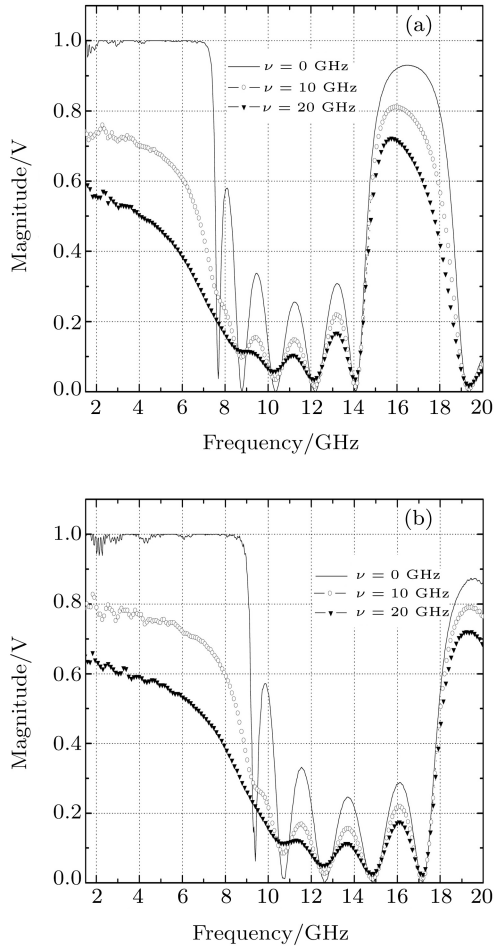


Fig. 6. Power reflection coefficients of the 2D-PPC with $\nu = 0$, 10 and 20 GHz at different incident angles, (a) $\theta = 30°$ and (b) $\theta = 45°$.

4. Conclusions

In this paper, an FDTD/PBC implementation is proposed by which EM wave transmission characteristic can be analysed for oblique incidence on 2D-PPCs. Then its validation is verified by comparing the reflection coefficient of the plasma slab using the algorithm with the analytic results. Finally, the reflection coefficients for the plasma photonic crystals using the FDTD/PBC algorithm are calculated to study the variation of bandgap characteristics with the incident angle and the plasma parameters. It is found that the incident angle may influence the bandgap, therefore, the influence of the incident angle must be taken into account while designing the PPC devices. For the effect of plasma frequency, we found that increasing the plasma frequency can broaden the bandwidth. Finally, for the effect of plasma collision frequency, we find that increasing the plasma collision frequency is impossible to broaden the bandwidth, on the contrary, it makes the photonic bandgap vanish gradually.

We only studied the characteristics of the 2D periodic structure, but in fact the FDTD/PBC algorithm can also be applied to analyse the 3D periodic structure and it is our next step of work. In addition, we can design more complex geometries using the FDTD/PBC algorithm to acquire excellent electromagnetic characteristics.

References

[1] Taflove A and Hagness S C 2005 *Computational Electrodynamics: The Finite-difference Time-domain Method* 3rd edn. (Boston: Artech House)

[2] Tsay W J and Pozar D M 1993 *IEEE Microwave and Guided Wave Letters* **3** 250

[3] Harms P, Mittra R and Wai K O 1994 *IEEE Trans. Antennas Propag.* **42** 1317

[4] Roden J A, Gedney S D, Kesler M P, Maloney J G and Harms P H 1998 *IEEE Transactions on Microwave Theory and Techniques* **46** 420

[5] Yang F, Chen J, Rui Q and Elsherbeni A 2007 *Radio Sci.* **42** RS4004

[6] Aminian A and Rahmat-Samii Y 2006 *IEEE Trans. Antennas Propag.* **54** 1818

[7] Lee J H and Kalluri D K 1999 *IEEE Trans. Antennas Propag.* **47** 1146

[8] Yang L X, Xie Y T, Wang Y J and Wang G 2009 *High Power Laser and Particle Beams* **21** 1710 (in Chinese)

[9] Yang L X, Wang Y J and Wang G 2009 *Acta Electron. Sin.* **37** 2711 (in Chinese)

[10] Yang L, Xie Y, Yu P and Wang G 2010 *Progress in Electromagnetics Research* M **12** 39

[11] Liu S B, Gu C Q and Zhou J J 2006 *Acta Phys. Sin.* **55** 1283 (in Chinese)

[12] Qi L M, Yang Z Q, Lan F, Gao X, Shi Z J and Liang Z 2010 *Acta Phys. Sin.* **59** 351 (in Chinese)

[13] Zhang H F, Ma L and Liu S B 2009 *Acta Phys. Sin.* **58** 1071 (in Chinese)

[14] Ma L, Zhang H F and Liu S B 2009 *Acta Phys. Sin.* **57** 5089 (in Chinese)

[15] Yang L X, Xie Y T, Kong W, Yu P P and Wang G 2010 *Acta Phys. Sin.* **59** 6089 (in Chinese)

[16] Brillouin L 2003 *Wave Propagation in Periodic Structures* 2nd edn. (New York: Dover Publications)

[17] Ginzburg V L 1970 *Propagation of Electromagnetic Waves in Plasma* (New York: Pergamon Press)